

Experimental and Computational Investigation of Viscoelasticity of Native and Engineered Ligament and Tendon

J. Ma, H. Narayanan, K. Garikipati, K. Grosh, and E.M. Arruda

Abstract The important mechanisms by which soft collagenous tissues such as ligament and tendon respond to mechanical deformation include non-linear elasticity, viscoelasticity and poroelasticity. These contributions to the mechanical response are modulated by the content and morphology of structural proteins such as type I collagen and elastin, other molecules such as glycosaminoglycans, and fluid. Our ligament and tendon constructs, engineered from either primary cells or bone marrow stromal cells and their autogenous matrices, exhibit histological and mechanical characteristics of native tissues of different levels of maturity. In order to establish whether the constructs have optimal mechanical function for implantation and utility for regenerative medicine, constitutive relationships for the constructs and native tissues at different developmental levels must be established. A micromechanical model incorporating viscoelastic collagen and non-linear elastic elastin is used to describe the non-linear viscoelastic response of our homogeneous engineered constructs *in vitro*. This model is incorporated within a finite element framework to examine the heterogeneity of the mechanical responses of native ligament and tendon.

1 Introduction

Ligaments and tendons are soft tissues that support muscle and bone structures in the body. The incidence of ligament and tendon rupture in the US has increased drastically in recent years; particularly acute among the pediatric population is the increased incidence of knee ligament rupture. A common autograph approach to anterior cruciate ligament (ACL) reconstruction uses a portion of the patient's patellar tendon as a graft. Previous investigations have shown differences in the viscoelastic responses of ligaments and tendons suggesting limitations in the ultimate efficacy

J. Ma, H. Narayanan, K. Garikipati, K. Grosh, and E.M. Arruda (✉)
University of Michigan,
e-mail: arruda@umich.edu

of a tendon as a ligament graft. Tendon allografts are also often used in ligament reconstruction; these incur an additional risk of immune rejection. These limitations have led to an increased urgency for engineered replacement tissues for ligament and tendon reconstructions. The goal of tissue engineering is to form viable constructs that can replicate the biomechanical function of native tissue, with biomechanically compatible interfaces between the engineered musculoskeletal tissue and native tissue. This requires detailed understanding of the function of native tissue and tissue interfaces, including growth and remodeling mechanics, structure – function relationships and healing response mechanics, to design optimal structures for skeletal tissue replacement. Therefore, the goal of our current tissue engineering approach is to develop self-organized, scaffold-free constructs for skeletal tissue replacement or reconstruction with mechanically viable, biochemically relevant tissue interfaces from patient-harvested cells, and to compare their mechanics at various developmental stages to the mechanics of native tissue.

Our laboratory has previously created engineered ligament, tendon and bone in vitro solely from bone marrow stromal cells (BMSC) or primary cells [6, 9, 15]. In order to evaluate the compatibility and feasibility of our in vitro experimental models, mechanical responses of native tissue under different conditions are investigated. Furthermore, computational models based on the finite element framework are established to examine the mechanics of both native and engineered soft tissue. Various mechanisms by which tissues respond to mechanical deformation have been observed, including non-linear elasticity, viscoelasticity and poroelasticity. Contributions to the overall mechanical response involve various known and unknown factors. In our computational model, factors that modulate the mechanisms include the content and morphology of structural proteins such as type I collagen and elastin, other molecules such as glycosaminoglycans, and fluid. Sufficient experimental data allow us to evaluate the accuracy and stability of the computational model.

Recently our laboratory has developed a scaffold-less method to co-culture three-dimensional (3D) ligament and bone constructs from rat BMSCs in vitro to engineer a bone-ligament-bone (BLB) construct [9]. Bone marrow was collected from rat femurs and tibias and cultivated to bone and ligament pathways using specific growth factors. Both types of cells were plated onto laminin coated culture dishes after the 3rd passage. After cells became confluent and the extracellular matrix that cells have synthesized was strong enough, bone monolayers were cut into two pieces and pinned using minutien pins on top of the ligament cell monolayers such that the proximal bone construct ends were 10 mm apart. Approximately 1 week following media change, the ligament monolayers rolled up around the bone constructs forming a 3-D BLB construct. These co-cultured constructs were used for ligament replacement in a rat model and the mechanics of these constructs were examined both prior to implantation and upon explantation. Briefly, the native MCL was excised and holes were drilled at the original MCL insertions on the bones. The engineered BLB construct replaced the native MCL by inserting its bone ends into corresponding holes. Four weeks of implantation of our BLBs in a medial collateral ligament (MCL) replacement application

demonstrated that our in vitro engineered tissues initially grew and remodeled quickly in vivo to an advanced phenotype and functionality to restore structural function to the knee [9]. Tangent moduli of the ligament portion of the BLB explants were equivalent to those observed in 14-day-old neonatal rat MCLs and this region stained positively throughout for crimped type I collagen and elastin. The explants also demonstrated viscoelastic and functionally graded responses that closely resembled those of native ligaments. We have also found that the average mechanical response is not sufficient to fully characterize the mechanical properties of ligament and tendon. Previous investigators have shown distinctly different bending strain response along different portions of native MCL [1, 16, 18]. These works have demonstrated higher strain levels near bone insertions compared to mid-ligament strains. Our investigations on native MCL have shown a heterogeneous mechanical response in tension that is consistent with the previous results. Results from our implantation showed the engineered BLB constructs adapted a functionally graded mechanical response in vivo that matched the heterogeneity of native MCL. Previously we have also shown functional inhomogeneity in rat tibialis anterior (TA) tendons [4]. Here we investigate this behavior in mice TA tendons from both adult and old animals. We develop a micromechanical model of non-linear viscoelasticity and implement it into a computational framework. We examine the efficacy of our computational model [6] to describe the functionally graded viscoelastic responses of native and engineered ligament and tendon.

2 Experimental Methods

This section briefly explains the native tissue isolation and mechanical testing methods. Details may be found in previous work [6, 9, 15].

2.1 Native Tissue Isolation

Fischer 344 rats were sacrificed at 14 days and 3 months following birth. The legs were dissected, removing the skin and muscle but maintaining the ligament connections at the knee. The MCL was isolated by removing all other knee ligaments. The tibia and femur were cut mid-bone to provide tissue for gripping during mechanical testing. C57Bl/6 mice were obtained at about 3 months and at 33–35 months and sacrificed. The feet were dissected and the TA tendon isolated as previously described [11]. The entire muscle–tendon–bone unit from the TA muscle to the first metatarsal bone was kept intact for gripping purposes so that the entire TA tendon, from the myotendinous junction (MTJ) to the enthesis, was in the field of view of the camera during mechanical testing.

2.2 Mechanical Evaluation of Native Ligament and Tendon

Cyclic tensile tests on native MCLs and TA tendons were conducted to obtain poroviscoelastic responses to multiple load/unload cycles and examine the mechanical heterogeneity of the ligament and TA tendon. Cross sectional areas (CSA) were measured from multiple locations along the samples. Multiple CSA measurements were taken at each region to obtain the average size of each region for future mechanical property measurements. An in-house designed tensiometer was employed to conduct the cyclic tension. The device consisted of an optical force transducer of our own design with a force resolution of 0.2–200 mN, two uniaxial servomotors controlled using Labview, and a Basler digital video camera connected to a Nikon (SMZ800) dissecting microscope [6]. Blue microsphere fiducial markers ($25\text{ }\mu\text{m}$ diameter) were brushed evenly on the surface of the samples for digital image correlation analysis of tissue displacements to provide highly accurate calculations of the tissue strain field along the entire sample. For strain reporting the TA tendon was partitioned into three approximately equal sub-regions, the distal or near-bone region, the fibrocartilage (FC) region (mid-section) and the proximal or near-muscle region. These three subsections are shown in Fig. 1. Ligament strain was measured across 2mm lengths near the insertions (Regions I and III) and at the mid-section (Regions II), as shown in Fig. 2. Samples were loaded in the device under cyclic tension loading (0–10% strain, 0.01 Hz) and the synchronized force and image recordings were compiled and controlled by LabVIEW software on a Dell Precision 300 computer. Load-unload cycles were conducted to characterize the overall non-linear poroviscoelastic response based on the average strain along the section length of the ligament and tendon. These same cyclic loading data were used with the local strain field measurements to examine the functionally graded response of the engineered or native ligament. Smoothed strain data were combined with the synchronized nominal stress (force over cross-sectional area) data to create the cyclic nominal stress vs. nominal strain response curves for each specimen.

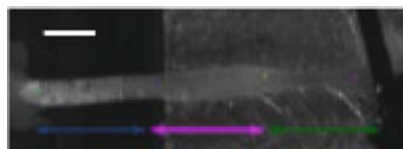
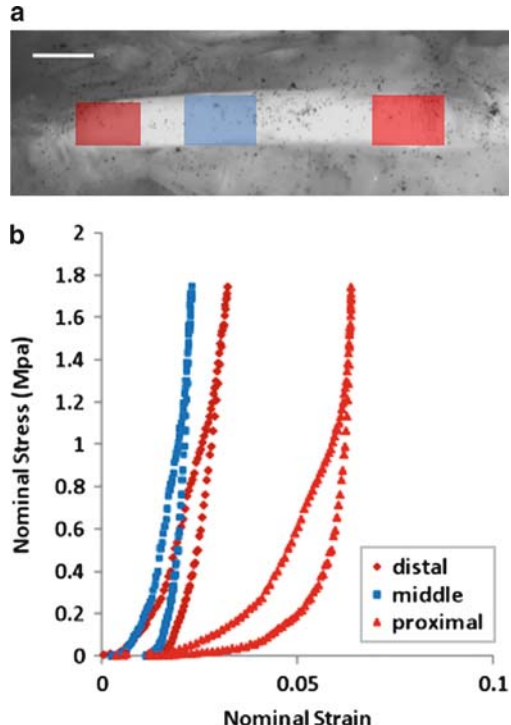


Fig. 1 Subsections of mouse TA tendon for strain reporting purposes: the proximal end (blue arrow) attached to muscle, the fibrocartilagenous mid-section (red arrow) and the distal end attached to bone (green arrow). Note that the TA muscle and metatarsal are held in the grips and the entire TA tendon strain field, from the MTJ to the enthesis, is examined. Scale bar = 1mm

Fig. 2 Native rat MCL mechanics at 3 months. (a) Strain analysis and (b) cyclic loading responses of I distal, II mid-section and III proximal regions



3 Mathematical Modeling of Mechanical Response

3.1 Micromechanical Modeling of Non-linear Viscoelasticity

The response of a homogeneous non-linear viscoelastic tissue is modeled in terms of the standard non-linear solid micromechanical model of Fig. 3. In this model, one non-linear spring B and linear viscous dashpot in series is in parallel with another non-linear spring A. To model the engineered and native tissue, a Gaussian or neo-Hookean chain network (see Treloar for example [17]) is used for spring A and a network of MacKintosh chains [10] is utilized in spring B. In this figure (Fig. 3), the nonlinear spring represents the entire 8-chain network of chains which is shown in Fig. 4.

As shown in Fig. 3 \mathbf{F}^e is the elastic part of the deformation tensor and \mathbf{F}^v is the viscous part. From compatibility, the total deformation \mathbf{F} can be derived as $\mathbf{F} = \mathbf{F}^e\mathbf{F}^v$. The left Cauchy Green Tensor \mathbf{B} is \mathbf{FF}^T . From equilibrium of the system, the total Cauchy stress tensor can be derived as $\sigma = \sigma_A + \sigma_B$, where σ_A is the Cauchy stress tensor generated from spring A and σ_B is the Cauchy stress tensor generated from spring B. The MacKintosh chain network of the micromechanical model is embedded within an initially isotropic or anisotropic 8-chain framework [2, 4, 5] as in Fig. 4 to mathematically model the mechanical behavior of ligaments and

Fig. 3 Micromechanical model of engineered and native tissue

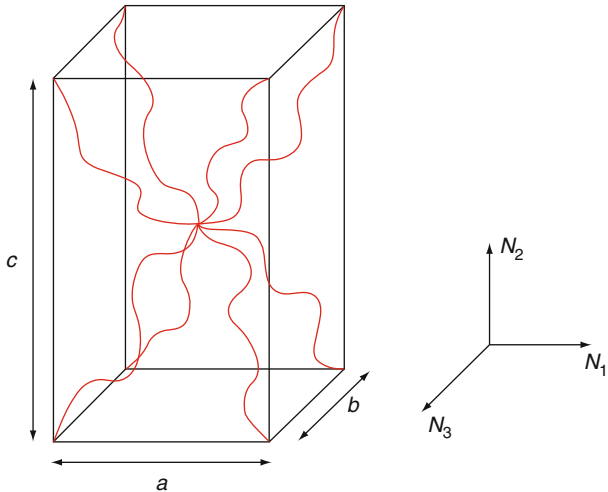
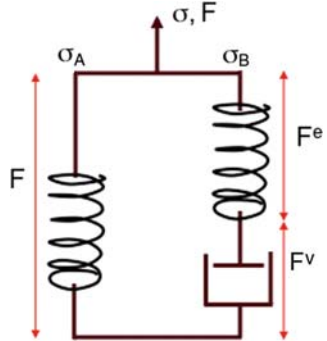


Fig. 4 An anisotropic representative volume element for a network of semi-flexible chains [4,5]

tendons. The Cauchy stresses on each element can be represented as follows:

$$\sigma_A = nk\Theta_A \mathbf{A}^e - p\mathbf{I} \quad (1)$$

$$\begin{aligned} \sigma_B &= \frac{nk\Theta_B}{3a} \frac{r_0}{\lambda_c} \frac{1}{4(1-\lambda_c\lambda_0/L_c)^2} \left(\frac{L_c/a - 6(1-\lambda_c r_0/L_c)}{L_c/a - 2(1-\lambda_c r_0/L_c)} \right) \mathbf{B} - p\mathbf{I}, \\ \lambda_c &= \sqrt{\text{tr}(\mathbf{B})}/3 \end{aligned} \quad (2)$$

In these constitutive equations, n is the chain density of the Gaussian or neo-Hookean and MacKintosh networks of chains, k is Boltzmann's constant, Θ is temperature, and p is the hydrostatic pressure. For the MacKintosh chain network a represents the persistence length, L_c represents the contour length, r_0 is the initial vector chain length and λ_c is the chain stretch. The linear dashpot constitutive

equation is $\mathbf{D}^v = \frac{\sigma'_B}{\eta^*}$ where \mathbf{D}^v is the viscous shear strain rate, η^* is the constant shear viscosity and σ'_B is the equivalent shear stress tensor. The network deformation is assumed to be isochoric and incompressible.

A rate formulation is employed to compute the stress vs. strain responses of various tissues to a cyclic load/unload test. Briefly, time and total stretch are prescribed so that \mathbf{F}^v can be explicitly computed based on the rate of deformation of the viscous dashpot updated from the previous step. \mathbf{F}^e is therefore updated in the current time step and then used to compute the stresses. Once the total stress is calculated, the rate of deformation is again updated for the viscous stretch computation in the next step.

3.2 Governing Equations of the Computational Model

Previously we were able to establish a multi-phasic computational framework for growth and remodeling in tissues to model a nonlinear anisotropic elastic or viscoelastic collagen network phase plus a fluid phase and various diffusing nutrients and soluble factors. This multiple species approach necessitates that classical balance laws are enhanced via fluxes of species relative to one another and sources e.g. of collagen to describe tissue growth [7, 12, 13]. In this way the model accounts for the coupled transport of species in a microstructurally evolving system subject to mechanical and chemical signals. The computational framework is required for the heterogeneous mechanical response (functional gradient) seen in native ligament and tendon as well as in engineered ligament explants.

The governing equations coupled with continuum balance equations describe the behavior of soft tissue as shown in Fig. 5. Constitutive laws are derived to satisfy the governing equations and are used to establish the finite element framework

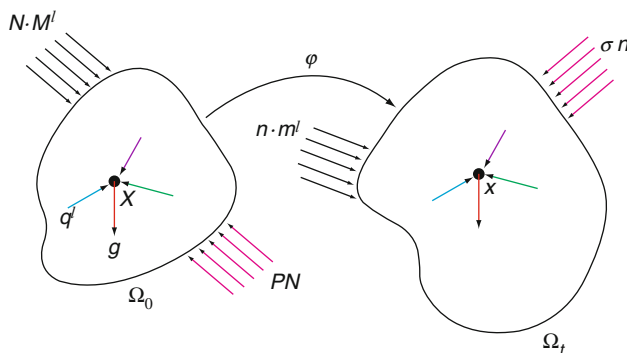


Fig. 5 Interaction forces, tractions and body forces on a tissue

to simulate the remodeling and ageing of soft tissue. Detailed derivations of the mathematical equations may be found in previous work [12, 13].

As a result of mass transport and the inter-conversion of species, the mass balance for an arbitrary species in the current configuration can be described as

$$\frac{\partial \rho^l}{\partial t} = \pi^l - \nabla_x \cdot m^l \quad (3)$$

where ρ^l is the species concentration, π^l is the species production rate and m^l is the species total flux. In soft tissues, the species production rate and flux are strongly dependent on the local state of stress. Therefore, the balance of linear momentum is coupled to mass transport in the determination of the local state of strain and stress which is described as follows:

$$\rho^l(g^l + q^l) + \nabla_x \cdot \sigma^l - (\nabla_x v^l)m^l \quad (4)$$

Quantities used in this equation are the g^l body force, q^l interaction force, σ^l partial Cauchy stress and v^l species velocity.

Summation over the rate of change of energy (1^{ST} Law) for all species in this system gives a result that insures there is no net energy production mechanism internal to the system. The energy equation is combined with the entropy inequality (2^{ND} Law), resulting in the Clausius–Duhem inequality, or reduced dissipation, which, along with constitutive assumptions, provides the constitutive laws. For instance, the internal energy of a species may assumed to be of the form:

$$e^l = \hat{e}^l(\mathbf{F}^l, \eta^l, \rho^l) \quad (5)$$

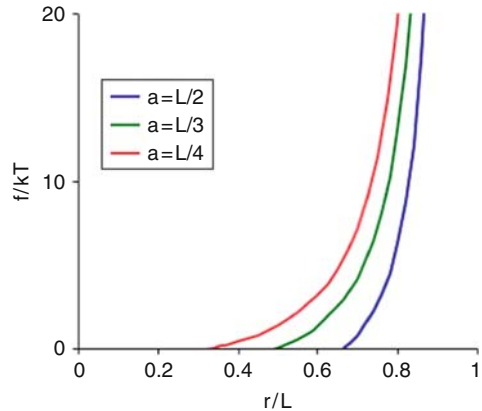
where \mathbf{F}^l is the deformation gradient, η^l is the entropy and the species concentration is ρ^l . Therefore the Clausius–Duhem inequality is derived as:

$$\begin{aligned} & \sum_l \left(\rho^l \dot{e}^l - \rho^l \dot{\eta}^l \theta - \sigma^l : \text{grad}(v^l) + \frac{\mathbf{h}^l \cdot \text{grad}(\theta)}{\theta} \right) \\ & + \sum_l \left(\rho^l (\mathbf{q}^l + \text{grad}(e^l)) - \text{grad}(\eta^l) \theta \cdot v^l + \pi^l \left(\psi^l + \frac{1}{2} \| v^l \|^2 \right) \right) \leq 0 \end{aligned}$$

where ψ^l is Helmholtz free energy and \mathbf{h}^l is the partial heat flux. Thermodynamically consistent constitutive relationships therefore arise from the dissipation inequality. For an elastic or viscoelastic material, a sufficient condition to satisfy is to specify that the partial second Piola–Kirchhoff stress tensor \mathbf{S}^c has the form

$$\mathbf{S}^l = \mathbf{F}^{e^{-1}} 2 \frac{\partial \hat{\psi}^l}{\partial \mathbf{C}^e} \mathbf{F}^{e^{-T}} \quad (6)$$

Fig. 6 The effect of persistence length on the force vs. extension response of a MacKintosh chain



with a suitable energy equation $\hat{\psi}^l$ for internal variables Γ_m of the collagen fibers. Since some compressible materials exhibit different bulk and shear responses, the free energy function is therefore decomposed into volumetric and isochoric parts:

$$\hat{\psi}^l(\mathbf{C}^e, \Gamma_1, \dots, \Gamma_m) = W_{vol}(J^e) + W_{iso}(\bar{\mathbf{C}}^e) + \sum_{\alpha=1}^m \gamma_\alpha(\bar{\mathbf{C}}^e, \Gamma_\alpha) \quad (7)$$

where J^e is the determinant of the elastic portion of the deformation gradient tensor and isochoric right Cauchy–Green deformation tensor $\bar{\mathbf{C}}^e = J^{e-2/3} \mathbf{C}^e$. The above equation has included the volumetric and isochoric equilibrium response of the solid phase and the viscoelastic response, characterized from the last term [12].

As shown in Fig. 6, variations in persistence lengths lead to differences in mechanical response. A smaller persistence length results in a longer toe region with a relatively compliant initial mechanical response, while a larger persistence length leads to a shorter toe region and a relatively stiffer response.

4 Results

4.1 Engineered Ligament In Vitro, In Vivo and Young Animal MCL

Uniaxial cyclic load/unload tests were conducted using in vitro and in vivo engineered BLB constructs and native neonatal rat MCL. The parameters of micromechanical model described previously were determined from the experimental results. The numerical and experimental results are shown in Fig. 7. By varying the stiffnesses of two nonlinear springs and the viscosity of the dashpot, the micromechanical model is robust enough to capture the mechanical responses of in vitro and in vivo engineered constructs and native MCLs.

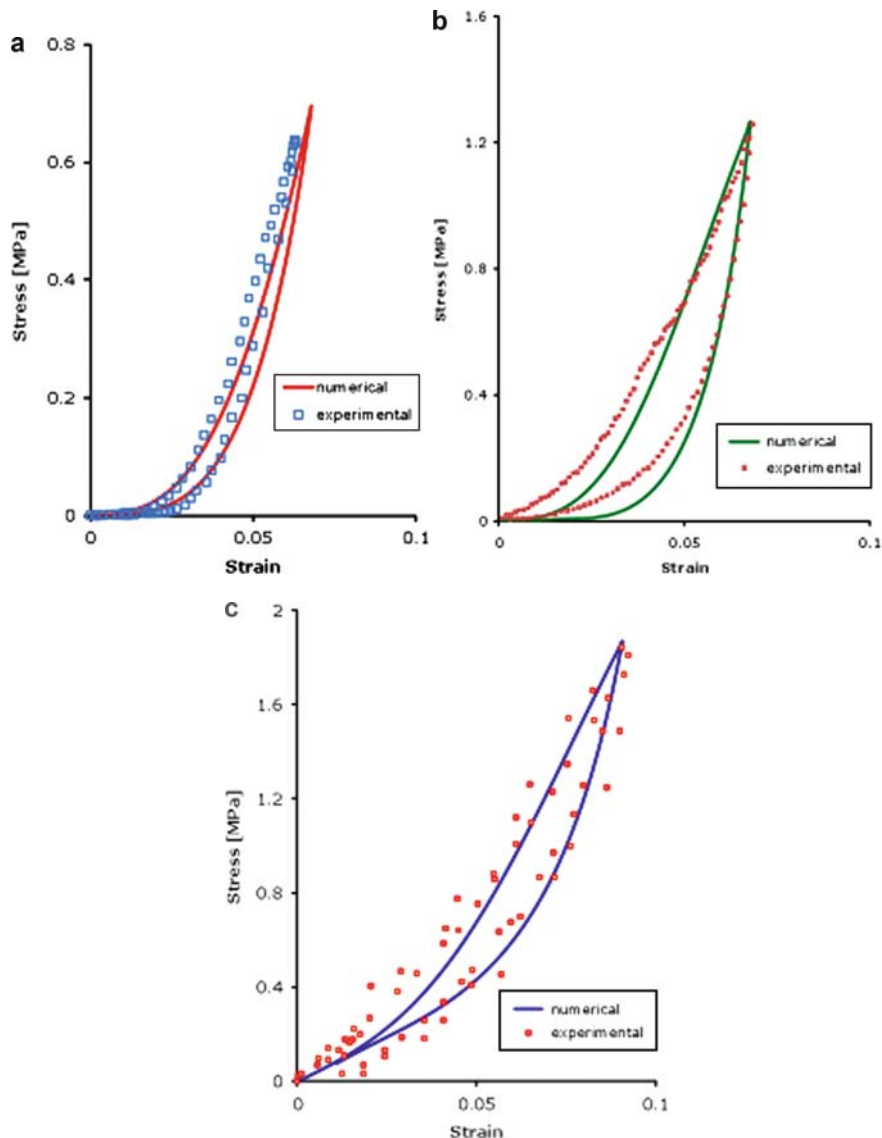


Fig. 7 Micromechanical modeling of engineered in vitro BLB constructs (a), engineered 1-month in vivo BLB constructs (b) and 14day old rat neonatal MCL (c)

4.2 Native Ligament and TA Tendon Mechanics

As shown in Fig. 2, our investigations of native MCL have found that the native ligament exhibits a heterogeneous mechanical response. Near either bone insertion the ligament is more compliant and more extensible and it exhibits appreciable

hysteresis (or viscous loss) during cyclic loading whereas along the mid-section the ligament is stiffer and less extensible and little hysteresis is seen. Functional heterogeneity is also found in adult mouse TA tendons. As shown in Fig. 8a, overall, the tendon demonstrates a viscoelastic response. Locally, the distal end is stiffer and

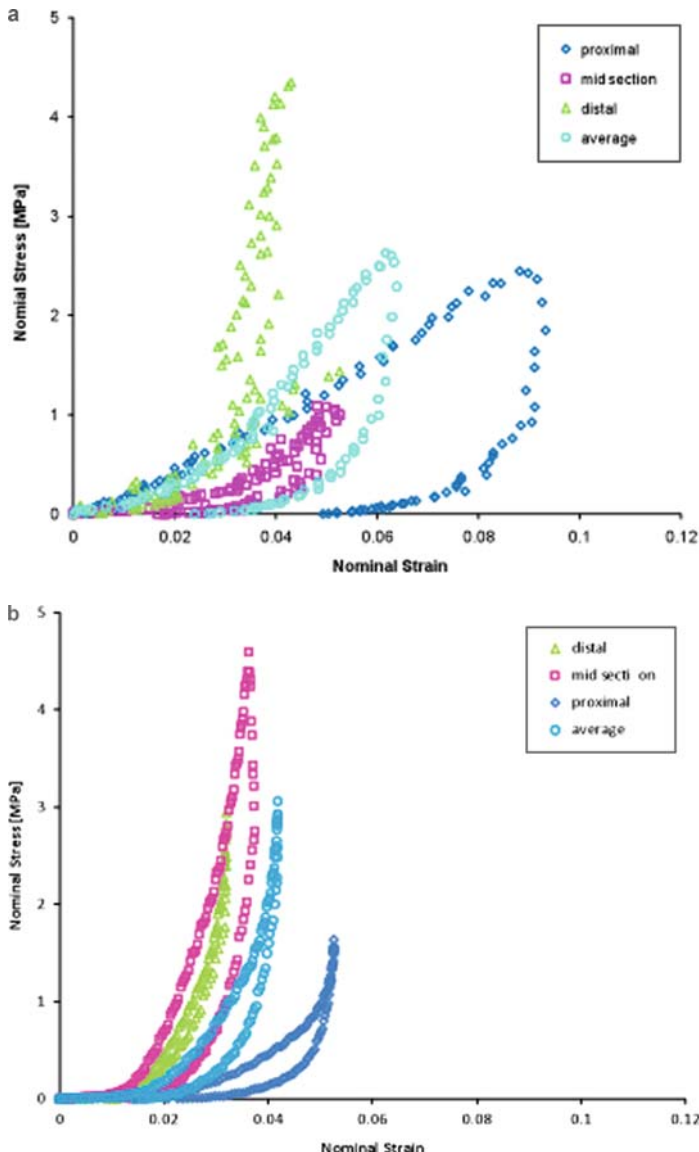


Fig. 8 Local mechanical response from experimental (a) & (b) and computational (c) and (d) results of adult and old TA tendons. (a) and (c) adult TA tendon, (b) and (d) old TA tendon

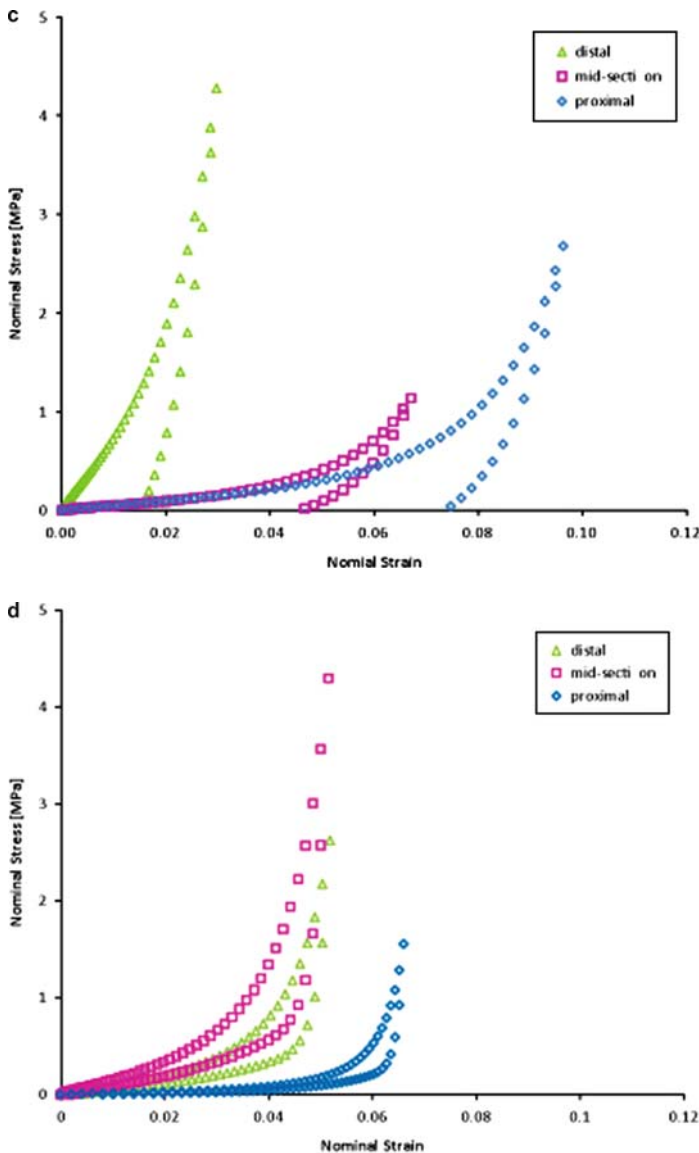


Fig. 8 (Continued)

less extensible than the proximal end, which is very compliant and extensible. Both the mid-section and the proximal end exhibit hysteresis, indicating a time dependent or viscoelastic behavior, whereas little hysteresis is seen at the distal end. A similar test protocol was conducted on old mouse TA tendon and the responses are shown in Fig. 8b. Ageing results in a leftward shift or stiffening in the response of the

mid-section and proximal end and therefore a decrease in the functionally graded mechanical response in old tendons. Hysteresis is also reduced in the mid-section and proximal end of old tendons.

4.3 Computational Results

The mathematical formulation developed for soft tissue has been implemented into a finite element framework using **COMSOL Multiphysics**, a computational environment for solving coupled systems of partial differential equations [12]. For simplification, the model is set up in a two dimensional structure assuming a state of plane strain. Triangular elements are used to characterize and estimate the displacement field of the soft tissue. Representative model geometries at the initial (undeformed) state are shown in Fig. 9. The mid-section of the adult TA tendon has the largest cross-sectional area whereas in the old TA tendon, this is the smallest section. Model geometries were chosen to approximate the cross-sectional area data. In order to model the functionally graded response of an adult TA tendon, the persistence length a was allowed to vary linearly in the simulation from the proximal end to the distal end whereas the contour length L_c , and the initial length r_0 were assumed to be constant along the tendon. In the old TA tendon much of the functionally graded extensibility has been lost and overall, the TA response is stiffer. This is modeled by a third order polynomial variation in a , a linear variation in l_p , a linear variation in r_0 , and constant contour length.

Parameters were fit from the experimental results and by varying the persistence lengths for different portions of TA tendons accordingly, the computational mechanical responses of adult and old TA tendons are obtained and shown in Fig. 8c and d. Compared to the corresponding experimental results, the model accurately captured several features of the overall mechanical response and the functional gradient of adult and old TA tendons with the same patterns that have been shown in the experimental data.

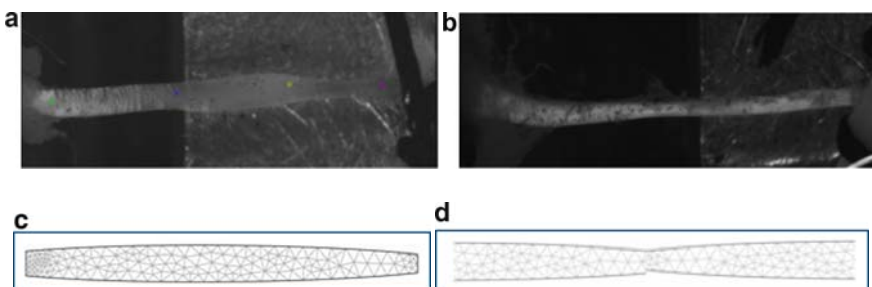


Fig. 9 TA tendon specimens from adult (a) and old (b) mice and representative initial model geometries for adult (c) and old (d) mouse TA tendons

5 Conclusion

Experimental results show the mechanical response of ligaments and tendons is non-linear, poroviscoelastic and functionally graded. Moreover, engineered ligaments used as an MCL replacement develop a functional gradient *in vivo*. Our computational model of connective tissue has been used to explore the rich mechanical response of native and engineered tendons and ligaments such as that of the TA tendon described above. Ageing was used as an example of how this computational model may also be used to examine constitutive property changes in tendon with disease and pathology. To replicate the complicated mechanical response of soft connective tissue with engineered materials is a challenge for tissue engineering.

References

1. Arms S, Boyle J, Johnson R, Pope M (1983) Strain measurement in the medial collateral ligament of the human knee: An autopsy study. *J Biomech* 16(7):491
2. Arruda EM, Boyce MC (1993) A three-dimensional constitutive model for the large stretch behavior of rubber elastic materials. *J Mech Phys Solid* 41(2):389
3. Arruda EM, Mundy K, Clave SC, Baar K (2006) Regional variation of tibialis anterior tendon mechanics is lost following denervation. *J Appl Phys* 53(4):1113–1117
4. Bischoff JE, Arruda EM, Grosh K (2002a) A microstructurally based orthotropic hyperelastic constitutive law. *J Appl Mech* 69:570–579
5. Bischoff JE, Arruda EM, Grosh K (2002b) Orthotropic hyperelasticity in terms of an arbitrary molecular chain model. *J Appl Mech* 69(4):198–201
6. Calve SC, Dennis RG, Kosnik P, Baar K, Groash K, Arruda EM (2004) Engineering of functional tendon. *Tissue Eng* 10(5,6):755–761
7. Garikipati K, Arruda EM, Grosh K, Narayanan H, Calve SC (2004) A continuum treatment of growth in biological tissue: Mass transport coupled with mechanics. *J Mech Phys Solids* 52(7):1595–1625
8. Larkin LM, Calve SC, Kostrominova TY, Arruda EM (2006) Structure and functional evaluation of tendon-skeletal muscle constructs engineered *in vitro*. *Tissue Eng* 12(11):3149–3158
9. Ma J, Goble K, Smietana M, Kostrominova T, Larkin L, Arruda EM (2008) Morphological and functional characteristics of three-dimensional engineered bone-ligament-bone constructs following implantation. *J Biomech Eng* (submitted)
10. MacKintosh FC, Kas J, Janmey PA (1995) Elasticity of semiflexible biopolymer networks. *Phys Rev Lett* 75:4425
11. Mendias CL, Bakhrurin KI, Faulkner JA (2001) Tendons of myostatin-deficient mice are small, brittle, and hypocellular. *PNAS* 105(1):388–393
12. Narayanan H (2007) Ph.D. Thesis: A continuum theory of multiphase mixtures for modelling biological growth, in Mechanical Engineering, University of Michigan, Ann Arbor
13. Narayanan H, Arruda EM, Grosh K, Garikipati K (2004) The micromechanics of fluid-solid interactions during growth in porous soft biological tissue. *J Mech Phys Solid* 52:1595–1625
14. Palmer JS, Boyce MC (2008) Constitutive modeling of the stress-strain behavior of F-actin filament networks. *Acta Biomater* 4:597–612
15. Syed-Picard FN, Larkin LM, Shaw CM, Arruda EM (2009) Three-dimensional engineered bone from bone marrow stromal cells and their autogenous extracellular matrix. *Tissue Eng Part A* 15(1):187–195

16. Thomopoulos S, Marquez JP, Weinberger B, Birman V, Genin GM (2006) Collagen fiber orientation at the tendon to bone insertion and its influence on stress concentrations. *J Biomech* 39:1842
17. Treloar LRG (2005) The physics of rubber elasticity. Oxford University Press
18. Warren LF, Marshall JL, Girgis F (1974) The prime static stabilizer of the medial side of the knee. *J Bone Jt Surg* 56(A):665